Infrared Spectroscopic Studies of Lyophilization- and Temperature-Induced Protein Aggregation

AICHUN DONG*, STEVEN J. PRESTRELSKI‡, S. DEAN ALLISON*, AND JOHN F. CARPENTER*x

Received September 6, 1994, from the *Department of Pharmaceutical Sciences, School of Pharmacy, Campus Box C238, University of Colorado Health Sciences Center, 4200 East Ninth Avenue, Denver, CO 80262, and ‡Amgen, Inc., Thousand Oaks, CA 91320. Accepted for publication November 7, 1994®.

Abstract □ Recent studies have clearly demonstrated that Fourier transform IR spectroscopy can be a powerful tool for the study of protein stabilization during freeze-drying and for optimizing approaches to prevent lyophilization-induced protein aggregation. The purpose of the current review is to provide an overview of these topics, as well as an introduction to the study of protein secondary structure with IR spectroscopy. We will start with a general summary of the theories and practices for processing and interpreting protein IR spectra. We will then review the current literature on the use of IR spectroscopy to study protein structure and the effects of stabilizers during lyophilization. Next we will concentrate specifically on protein aggregation. The bulk of the research and the key assignments of spectral features in protein aggregates come from studies of the effects of high and low temperature on proteins. Therefore, we will first consider this topic. Finally, we will summarize the recent theoretical and applied work on lyophilization-induced aggregation.

When a protein product is not sufficiently stable in aqueous solution, lyophilization or freeze-drying is the method most commonly used to prepare the protein for long-term storage. However, often the acute freezing and drying stresses of lyophilization irreversibly damage the protein. The damage is manifested as denaturation and aggregation when the protein sample is rehydrated. Thus, the advantages of storing a protein product in the dried solid cannot be exploited unless the acute damage arising during lyophilization is inhibited. Numerous empirical studies have documented that when certain stabilizers (e.g., sugars) are added to protein formulations, native, functional proteins can be recovered upon rehydration. More recently, we have documented that it is necessary to add solutes that stabilize against both the freezing and drying stresses to assure protection of the protein.[1-3] The mechanisms by which various stabilizers protect proteins during freezing and drying have recently been reviewed[4] and will not be covered here. Rather, in the current review we will discuss the structural basis for lyophilization-induced aggregation and for the prevention of aggregation with protein stabilizers, and the utility of using IR spectroscopy to study these phenomena.

Until recently, the only way to assess the capacity of an additive to stabilize a protein during lyophilization was to measure activity and/or structural parameters after rehydration. Due to a lack of appropriate methodology to detect conformational changes of proteins under various physical conditions (i.e., in the dried solid as well as in aqueous solution), freezing- and drying-induced changes in protein structure were unknown. To confound matters further, it was proposed in the literature on protein chemistry that dehydration did not alter the conformation of a protein.[5] Such a claim was clearly counter to the known contributions of water to the formation of the native, folded protein.[6,7] Also, it was difficult to reconcile the finding that proteins could be irreversibly inactivated and aggregated after rehydration with the contention that protein structure was not perturbed by dehydration.

Reconciliation of this apparent dilemma was provided by Fourier transform IR (FT-IR) spectroscopy, which can be used to study protein secondary structure in any state (i.e., aqueous, frozen, dried, or even as an insoluble aggregate). By applying powerful methods of second-derivative and correlation coefficient analysis (see below) to the protein spectra, Prestrelski and colleagues[2,3] unequivocally demonstrated that dehydration can induce protein unfolding. Their comparison of the second-derivative spectra of several proteins in aqueous solution to the respective spectra for the proteins in the dried solid led to several conclusions: (1) Dehydration-induced spectral alterations in the conformation-sensitive amide I region were due to protein unfolding and *not* simply to the loss of water from the protein. The intrinsic effects of water on the vibrational properties of the peptide bond, and hence protein IR spectra, were insignificant. (2) With γ-interferon, lyophilization-induced unfolding resulted in aggregation during rehydration. (3) Finally, prevention of aggregation and recovery of activity of labile enzymes after rehydration correlated directly with retention of the native structure in the dried solid. That is, the mechanism by which stabilizing additives (e.g., sugars) protect proteins during lyophilization is to prevent unfolding.

Based on this and subsequent studies reviewed below, it is clear that FT-IR spectroscopy has great potential for application in the study of protein stabilization during freeze-drying and in optimizing approaches to prevent lyophilization-induced protein aggregation. The purpose of the current review is to provde an overview of these topics as well as an introduction to the technique. We will start with a general summary the theories and practices of processing and interpreting IR data on protein structures. We will then review the current literature on the use of IR spectroscopy to study protein structure and the effects of stabilizers during lyophilization. Next we will concentrate specifically on the study of protein aggregation. The bulk of the research and the key assignments of spectral features in protein aggregates come from IR studies of the effects of high and low temperature on proteins. Thus, we will first consider this topic. Finally, we will summarize the recent theoretical and applied work on lyophilization-induced aggregation.

Theoretical Background of IR Data Processing—IR spectroscopy has long been a favored technique for structural and functional investigations of biomolecules. One of the advantages of the method is its ability to monitor the structural changes of polypeptides and proteins under various physical conditions including: aqueous solutions,[8-12] cast films,[13] dried solids,[2,3,14] or aggregates.[15,16] Advanced by computerized Fourier transform instrumentation and powerful mathematical band-narrowing techniques that enhance spectral resolution (namely, Fourier self-deconvolution and second-derivative analysis) IR spectroscopy has been widely used to study the secondary structure of polypeptides and proteins in the past few years. The reader is directed to the

® Abstract published in *Advance ACS Abstracts,* February 15, 1995.

0022-3549/95/3184-0415$09.00/0

papers by Susi and Byler,[8] Surewicz and Mantsch,[9] Krimm and Bandekar,[17] and Bandekar[18] for general reviews on the application of IR to the study of protein structure and the relative merits of working in H_2O versus in D_2O.

The vibrational spectra of protein molecules are determined by their three-dimensional structures and the vibrational force fields. An analysis of these spectra can, therefore, provide information on structures and on inter- and intramolecular interactions. Protein molecules exhibit many vibrational frequencies. Nine characteristics group frequencies arise from the peptide linkages. These have been identified as: amide A (~3300 cm^{-1}), amide B (~3100 cm^{-1}), amide I (~1650 cm^{-1}), amide II (~1550 cm^{-1}), amide III (~1300 cm^{-1}), amide V (~735 cm^{-1}), amide IV (~635 cm^{-1}), amide VI (~600 cm^{-1}), and amide VII (200 cm^{-1}).[17,19] These amide vibrational bands can be described in terms of five in-plane (C=O stretching, C—N stretching, N—H stretching, OCN bending, and CNH bending) and three out-of-plane (C—N torsion, and C=O and N—H bendings) displacement coordinates.[17]

The amide I band is sensitive to small variations in molecular geometry and hydrogen bonding patterns within proteins. This band is due primarily to the C=O stretching vibrations of the peptide linkages that constitute the backbone structure of proteins, combined with small contributions from the out-of-phase C—N stretching and C—C—N bending vibrations.[17] The lack of major interfering bands from other structures in proteins and peptides makes the amide I band the most useful of the amide bands for assessing protein structure. One potential difficulty is that the side-chains of several amino acids also absorb in the amide I region. In practice, however, significant effects of residue side-chain absorption on protein secondary structure estimation have not been found.[8,16] There are two possible reasons for this result. First, side-chain absorptions are generally weak, broad, and distributed widely within the amide I region. That is, the intensity of side-chain absorbance relative to that of peptide amides is not significant. Second, the spectral contributions of side-chains appear to be different in free amino acids from that in the protein/peptide microenvironment. An extreme example is seen with poly-L-lysine. The 1630 cm^{-1} absorbance observed for the side-chains of free lysine is not observed in the second-derivative spectra of poly-L-lysine.[3]

The amide I band has been used extensively in studies of secondary structural composition and conformational changes of proteins.[8-12,18-20] Each type of secondary structure (i.e., α-helix, β-sheet, turn, and unordered structures) gives rise, in principle, to a different C=O stretching frequency in the amide I region of the IR spectrum. The different frequencies are due to differences in intermolecular interactions, mainly the hydrogen bonding patterns. An analysis of the amide I band components can provide quantitative as well as qualitative information about the secondary structure of the proteins. However, a major problem in the IR study of protein conformations is the intrinsically broad bandwidth of the amide I components that arise from the various secondary structures. The bandwidths of these overlapping components are often greater than the separation between the absorbance maxima of adjacent bands. Hence, the amide I absorbance usually appears as a single broad band contour. Because the band overlapping is beyond the instrumental resolution, several mathematical band-narrowing methods have been developed to overcome this problem.[8,21-25] These methods are critical to the application of FT-IR in the study of protein structure and, hence, will be explained briefly. We will first describe the major methods used to resolve overlapping bands for qualitative assignment to given secondary structural types. Next, we will critique the relative merits of each method for quantitation of the proportion of each secondary structural type in a protein.

Deconvolution—Fourier self-deconvolution (FSD) was first described by Stone[21] and then discussed further by Kauppinen and colleagues.[22,23] The basic theoretical consideration of FSD is that a "true" profile of an IR vibrational band can be approximated as a Lorentzian function and expressed mathematically as follows:[22,26]

$$A(\nu) = A_0\gamma^2/[\gamma^2+(\nu-\nu_0)^2] \quad (1)$$

where $A(\nu)$ is the band absorbance at wavenumber ν, A_0 is the maximum absorbance of the band, ν_0 is the wavenumber for A_0, and γ is the half-width at half-height (HWHH). The cosine Fourier transform of $A(\nu)$ is given by:

$$I(x) = F\{A(\nu)\} = \int_0^\infty A(\nu)\cos(2\pi\nu x)\,d\nu = 1/2A_0\,\gamma\cos(2\pi\nu_0 x)\exp(-2\pi\gamma x) \quad (2)$$

where x is a spatial frequency with units of centimeter when ν has the units of cm^{-1}. Because the exponential decay term $\exp(-2\pi\gamma x)$ is determined by the half-width of the vibrational band, decreasing the rate of decay in the Fourier domain will reduce the bandwidth in the frequency domain. This can be achieved by multiplying $I(x)$ with an exponentially increasing function $D(x) = \exp(2\pi Dx)$:

$$I'(x) = I(x)\cdot\exp(2\pi\gamma x)\cdot Dx = 1/2\cdot A_0\gamma\cos(2\pi\nu_0 x)\cdot Dx \quad (3)$$

Because the reverse Fourier transformation is performed on $I'(x)$, a narrower band $A'(\nu)$ is obtained. The enhance factor (K value) is defined as $K = \gamma/\gamma'$.

Derivative Spectroscopy—An alternative approach for the separation of overlapping bands is to obtain the nth-order derivative of an absorption spectrum. Derivative analysis can be performed on either the Fourier domain[25] or the frequency domain.[8,24] The second-order derivative is most commonly used. One major advantage of this method is that it is completely objective; there is no need to choose values for subjective parameters, as there is for FSD (see below).

In the Fourier domain derivative, a spectrum $A(\nu)$ and its Fourier transform $I(x)$ are related by the following equation[25]:

$$A(\nu) = F\{I(x)\} = \int_0^\infty I(x)\cos(2\pi\nu x)dx \quad (4)$$

The second-order derivative is given by:

$$d^2A(\nu)/d\nu^2 = \int_0^\infty(-2\pi x)^2 I(x)\cos(2\pi\nu x)dx \quad (5)$$

In the frequency domain derivative, the second-order derivative of spectrum is given by the following[8,24]:

$$A^{II} = -(1/\pi\gamma)[2a(1-3a\nu^2)/(1+a\nu^2)^3] \quad (6)$$

where γ is the half-width at half-height and a equals $1/\gamma^2$. The peak frequency of the second derivative is identical with the original peak frequency. The half-width of the second derivative is related to the half-width of the original line by $K = \gamma/\gamma^{II} = 2.7$, and the peak intensity of the second derivative is related to the original intensity by $A_0^{II} = -2A_0/\gamma^2$.

A major factor preventing the bandwidth of a spectrum from being reduced beyond certain limits, by either deconvolution or derivative analysis, is the rapid degradation of the signal-to-noise (S/N) ratio of the spectrum. Both procedures will amplify disproportionately the weak features in the spectrum, which originate from random noise and uncompensated water vapor. Therefore, the importance of obtaining a high quality IR spectrum can never be overemphasized. Random noise from thermal radiation of the surroundings is always present

in a recorded spectrum, due to the electronic devices being operated above absolute zero temperature. However, the multiplex (Fellgett) advantage of FT-IR instrumentation and computerized averaging of multiple spectra can greatly increase the S/N ratio of the recorded spectrum. In turn, the effect of random noise is minimized in subsequent mathematical band-narrowing.

The most troublesome "noise" comes from the absorbance bands of uncompensated atmospheric water vapor, which generally cannot be smoothed away mathematically without distorting the spectrum of protein. Unfortunately, the recorded spectrum always contains bands from water vapor. The vapor remains in the IR radiation path, even under extensive dry air or nitrogen gas purging. However, the spectral signals of water vapor are independent from the signals of protein and liquid water. Therefore, the bands from water vapor can be satisfactorily eliminated from the observed protein spectrum by subtracting a water vapor spectrum.[12,27] In practice, the "degree of subtraction" is determined iteratively by subtracting the vapor spectrum until the protein spectrum is smooth in the region between 1850 and 1720 cm^{-1}. This procedure can be carried out with either the original spectrum or its second derivative. Often, it is much easier to remove the water vapor components from the second-derivative spectrum than from the original spectrum.

Merits of FSD and Second Derivative Methods in Studies of Protein Structure Perturbations—Quantitative comparisons of lyophilization-induced and thermally-induced conformational changes of proteins present challenging problems for investigators. First, there is no corroborating information (e.g., from X-ray crystallography) available on protein structures that differ dramatically from the native state. Second, changes in protein conformation result unavoidably in changes in the frequencies and widths of the component bands that make up amide I IR spectra. Under these circumstances, the choice of a suitable band-narrowing technique is as important as data interpretation.

There are a number of factors to consider when comparing the relative utility of FSD versus the second-derivative method for the analysis of protein spectra. First, both techniques work equally well in resolving overlapping protein amide I components. Often the deconvoluted spectrum appears more attractive than the second derivative, because with the former method there is a visual correlation between resultant and original bands. Second, in combination with curve-fitting, both techniques have been used successfully in quantitative analysis of protein secondary structures.[8,12,28–30] As an example, the amide I spectrum of β-lactoglobulin B and the fitted curves for FSD and second-derivative spectra are shown in Figure 1. For easier comparison, the second derivative is inverted by multiplying by −1. Assignments of the amide I band components to secondary structural elements can be made based on previous reports.[8,12,31] Curve-fitting and quantitative analysis gives 50.6% β-sheet, 10.5% α-helix, 20.4% turn, and 18.5% unordered by the FSD method[8] and 54.5% β-sheet, 9.4% α-helix, 19.2% turn, and 16.9% unordered by the second-derivative method.[29] The results from both methods agree closely with the result of X-ray crystal analysis (53% β-sheet and 7% α-helix).[32,33]

A major drawback of the FSD method, the most popular approach for quantitative analysis of amide I components, is that the choice of values for the two key parameters (half-bandwidth and enhance factor) is arbitrary and highly subjective because of the lack of knowledge of the real values, as well as because the component bands may have unequal half-bandwidths. As a result, by varying input parameters, substantially different FSD spectra can be generated from the same IR spectrum.. As shown in Figure 2, changing either the enhance factor or the half-bandwidth can lead to changes

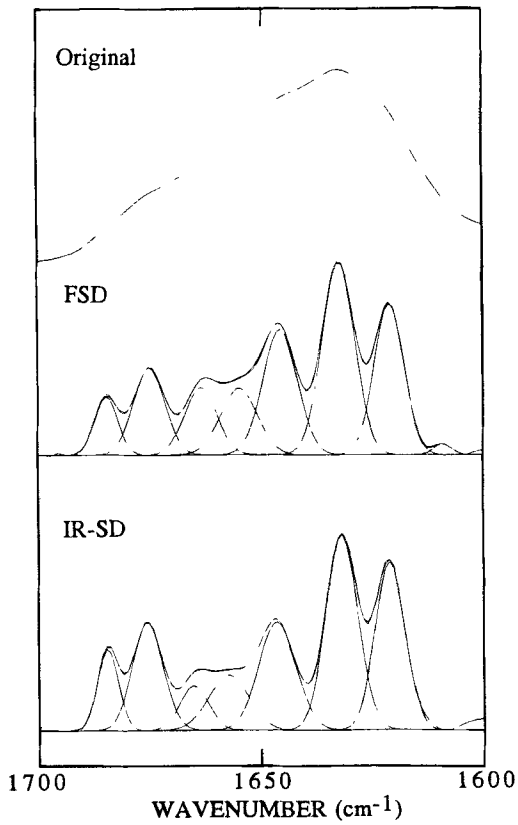

Figure 1—The original, Fourier self-deconvoluted, and inverted second-derivative spectra of β-lactoglobulin B (10 mg/mL) in 10 mM phosphate/D_2O buffer (pD 7.0): (top) the original spectrum; (middle) the curve-fitted FSD spectrum (half-bandwidth 23 cm^{-1}, $K = 2.7$); (bottom) the curve-fitted inverted second-derivative spectrum (Dong, A.; Matsuura, J.; Allison, S. D.; Chrisman, E.; Manning, M.; Carpenter J. F., unpublished results).

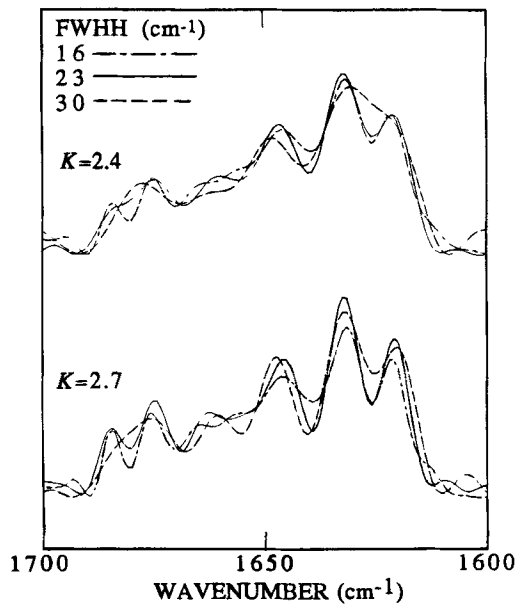

Figure 2—Effects of input parameter variations on the amide I spectrum of β-lactoglobulin B by Fourier self-deconvolution. β-lactoglobulin B (10 mg/mL) in 10 mM phosphate/D_2O buffer (pD 7.0) after 24 h H-D exchange. The spectrum was recorded on a Magna IR model 550 (Nicolet) with a 4 cm^{-1} resolution at 25 °C.

in the total number of component bands resolved, as well as alterations in the peak frequency of the bands. Probably most important for the study of protein structural perturbations,

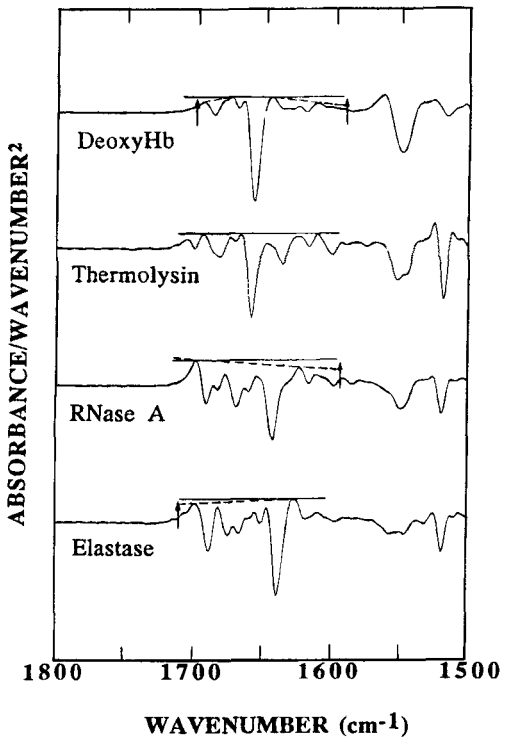

Figure 3—Examples of non-zero baseline selection for the second-derivative amide I spectra of proteins. The dashed lines represent the non-zero baseline selected, and the solid lines represent the position of baseline after correction (taken from unpublished protein database of A. Dong, P. Huang, B. Caughey, J. F. Carparter, and W. S. Caughey).

the bandwidth relations are lost in the FSD as a result of arbitrary bandwidth input.[34] To make a meaningful comparison between two spectra with FSD, one must use the same input parameters for both spectra. However, it is apparent from several studies[2,3,15] that the bandwidths of amide I components of lyophilized or thermally denatured proteins are much broader than those for the native proteins. Thus, it is difficult to deconvolute the spectra of native and unfolded proteins in a manner that allows meaningful quantitative comparisons to be made. In practice, by using the same input parameters (see below), qualitative comparisons can be, and often are, made to reveal changes in frequencies of the component bands of a protein during a treatment (e.g., thermal unfolding and aggregation).

It has been proposed that the second-derivative method cannot possibly be used as a quantitative tool in the analysis of the protein amide I band.[35] However, the results from studies of >35 globular proteins with known X-ray crystal structures provide evidence that the refined second-derivative method[29] is comparable to or even better than other methods in estimating secondary structure of proteins.[36] It is generally stated that the integrated intensity is lost in the second derivative[34] because the integrated intensity of a derivative function equals zero. However, the intensity relations between a second-derivative and an original spectrum are generally retained, if only the center band area (with a non-zero baseline) of the second derivative is utilized (see Figure 1). The non-zero baseline can be obtained easily by connecting two (up to four in the cases of proteins containing >60% α-helical structure; e.g., myoglobin) most positive points within the amide I region (Figure 3). With the baseline assigned, the relative areas of the component bands in the second-derivative spectrum can be determined by a curve-fitting procedure.[29,30] Thus, the general retention of bandwidth relations and relative band areas between the original

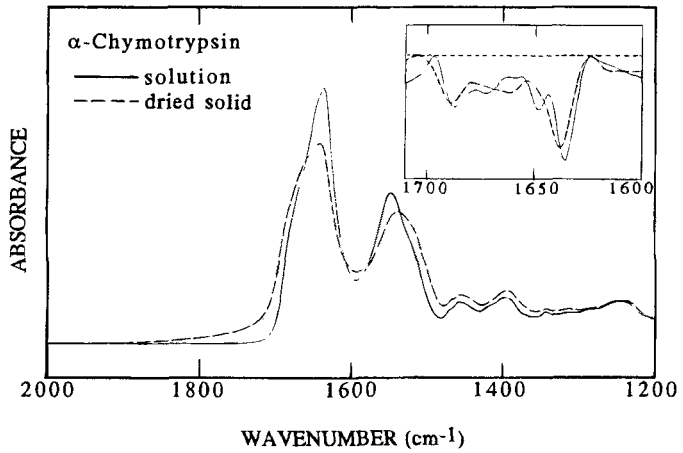

Figure 4—Comparison of IR spectra of α-chymotrypsin in aqueous and dried solid states. The insert shows the second derivatives in the amide I region of the spectra in the main panel.

Table 1—Assignments and Relative Areas of Amide I Components of α-Chymotrypsin in Aqueous Native and Dried States[a]

Aqueous Solution		Dried Solid		
ν(cm^{-1})	Area (%)	ν(cm^{-1})	Area (%)	Assignment
1635	37.9	1638	38.1	β-Sheet
1648	16.3	1648	9.1	Unordered
1658	7.3	1659	12.5	α-Helix
1668	6.9	1668	11.3	Turn
1675	10.3	1677	7.8	Turn
1683	9.8	—	—	Turn
1689	11.5	1689	21.0	β-Sheet

[a] The band components between 1620 and 1600 cm^{-1}, which arise from side-chain vibrations, are not included in calculation.

spectrum and its second derivative permit the usage of second derivative in quantitative as well as qualitative spectral analysis.

On the other hand, second-derivative analysis also has inherent shortcomings, including the potential interference of weak positive side lobes associated with the second derivative and the dual relations between the peak height of the second-derivative spectrum and the peak height and width of the original spectrum. The latter shortcoming may cause considerable distortions in the relative band areas when strong, sharp bands are mixed with weak, broad bands. This is especially problem when amide I component bands are already visually identifiable, prior to mathematical band narrowing. We found this to be the case with the spectra of some short peptides.[3]

A major advantage of the second-derivative method is that subjective input of arbitrary parameters is not needed. More importantly, quantitative analysis with second-derivative spectra can be performed even when the bandwidths of amide I components change during the course of an experiment (e.g., lyophilization-induced or thermally-induced protein unfolding and aggregation). The original and second-derivative spectra of α-chymotrypsin in aqueous and dried states are shown in Figure 4. Results of quantitative analysis by curve-fitting to the inverted second-derivative spectra are give in Table 1. The results for the aqueous native state agree closely with those from X-ray crystallographic analysis: 50.4% β-sheet, 10.6% α-helix, 24.6% turn, and 14.4% unordered structures.[38] Lyophilization induces small changes in the relative proportions of secondary structures. There is a reduction in the percentages of disordered and turn structures and an increase the content of β-sheet and α-helix. Even though these quantitative changes are rather modest, it is clear from the overall

alterations in band shapes and positions that the protein is non-native in the dried solid.

Such alterations, which reflect "global" changes in the spectrum, can be quantified with an alternative approach for comparing two second-derivative spectra. Prestrelski and colleagues[2,3] have developed a mathematical procedure to calculate the spectral correlation coefficient (similarity) between two second derivative spectra:

$$r = \frac{\sum^{n} x_i y_i}{\sqrt{\sum x_i^2 \sum y_i^2}} \quad (7)$$

where x_i and y_i are the spectral absorbance values of the reference and sample spectra respectively, at the ith frequency position in the amide I region. The correlation coefficient between two spectra of a given protein equals 1 when there is no conformational change in the protein. The larger the change in conformation, the greater are the differences between the spectra and the smaller is the value for r. The variability of r values for the spectra of several proteins, recorded in duplicate under identical conditions, is insignificant.[2,3] Correlation coefficient analysis has proven valuable in quantitative evaluation of lyophilization-induced structural changes in proteins. For example, the recovery of activity of lactate dehydrogenase after lyophilization and rehydration correlated directly with the r value for the spectrum of the protein in the dried solid versus that for the native, aqueous state.[3]

Temperature-Induced Protein Aggregation—The utility of FT-IR spectroscopy for studying protein aggregation has been demonstrated most extensively in studies of thermally-induced aggregation. Thus, before considering IR studies of lyophilization-induced aggregation, it is useful to review thermal studies to gain insight into the connection between unfolding and aggregation, as well as into the interpretation of IR spectra of protein aggregates.

In the first reported IR study of protein aggregation, Clark and colleagues[15] work with proteins in a D_2O solution and used a dispersive IR spectrometer. They monitored the spectral changes in the amide I region of five globular proteins [bovine serum albumin (BSA), lysozyme, insulin, ribonuclease, and α-chymotrypsin] as a function of temperature between 25 and 95 °C. At temperatures >60 °C, they observed a new well-defined amide I band around 1620 cm^{-1} (without use of mathematical band-narrowing techniques) for all five proteins. As temperature increased, the intensity of the 1620 cm^{-1} band increased at the expense of other band components. This intense band was retained after cooling. The proteins were irreversibly aggregated, indicating that the 1620 cm^{-1} band was due to protein aggregates. This suggestion was substantiated by the observation that the growth of the 1620 cm^{-1} band in the spectrum of BSA during heating correlated with changes detected by small-angle X-ray scattering, which were indicative of the formation of a intermolecular and/or intramolecular network.[39] On the basis of earlier IR studies on fibrous proteins by Miyazawa and Blout[40] and Krimm,[41] and on the thermally-induced α-helix-to-β-sheet transition of poly-L-lysine,[42] Clark and colleagues assigned the 1620 cm^{-1} band to a strongly hydrogen-bonded, antiparallel β-sheet structure (i.e., intermolecular β-sheet in protein aggregates).

In subsequent studies, much more detailed IR spectral changes in the amide I region of proteins were revealed by high sensitivity FT-IR instruments and mathematical band-narrowing techniques. Casal and colleagues[43] investigated the conformational changes of β-lactoglobulin B at various pH and temperature conditions by FSD IR spectroscopy. They heated the protein solution from 20 to 90 °C and recorded the IR spectra at intervals of ~6 °C. As shown in Figure 5, the

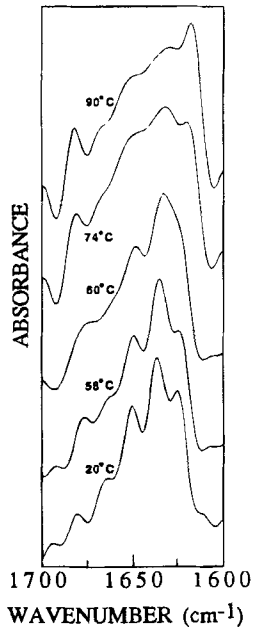

Figure 5—The Fourier self-deconvoluted amide I spectra of β-lactoglobulin B in 50 mM phosphate/D_2O buffer (pH 7) recorded at indicated temperatures. Reproduced from Casal et al.[43]

spectra obtained at 20 and 58 °C were essentially the same. Both contained bands at 1694, 1680, 1664, 1649, 1636, and 1624 cm^{-1}. However, the spectra recorded at 60, 74, and 90 °C revealed remarkable changes. The first stage of thermal unfolding was represented by the spectrum recorded at 60 °C, which contained bands at 1675, 1648, and 1633 cm^{-1} and a shoulder around 1620 cm^{-1}. The final stage of the thermally-induced unfolding and aggregation was represented by the spectrum recorded at 90 °C, which contained bands at 1682, 1667, 1650, 1632, and 1620 cm^{-1}. The bands at 1620 and 1682 cm^{-1} were both characteristic of the intermolecular β-sheet in the protein aggregates. Taken together, these results indicate that thermally-induced unfolding precedes aggregation.

Using second-derivative IR spectroscopy, Byler and Purcell[44] studied the thermal unfolding of β-lactoglobulin, α-lactalbumin, and BSA in D_2O solutions. The second-derivative spectra of BSA obtained at 30, 61, 80, and 92 °C are shown in Figure 6. The native BSA contains predominantly α-helix, which give rises to the strong absorbance around 1651 cm^{-1}. When heated above its unfolding temperature (~75 °C), BSA exhibited a new, strong low-frequency β-sheet component at 1613 cm^{-1}, accompanied by a weak band at 1684 cm^{-1}. Although greatly diminished in intensity, the presence of band at 1651 cm^{-1} in the spectrum recorded at 90 °C indicated that not all of the α-helical structures uncoiled in the course of unfolding and aggregation.

The thermally-induced aggregation of several other proteins [azurin,[45] cholera toxin,[46] adenylate cyclase,[47] cytochrome c,[48] chymotrypsinogen,[49] concanavalin A,[50] acetylcholine receptor,[51] glucoamylase,[52] acetylcholinesterase,[53] transglutaminase,[54] ribonuclease T1,[55] and ribonuclease A[56]] has also been studied by FSD or second-derivative IR spectroscopy in the past few years. In all of these studies, a common feature of thermally-induced protein aggregates is the formation of an intermolecular hydrogen-bonded antiparallel β-sheet structure, represented by the low-frequency band around 1620 cm^{-1} and associated weaker high-frequency band around 1685 cm^{-1}. This structural transition occurs regardless of the initial secondary structural composition of the native proteins.

The other common feature of thermally-induced unfolding revealed by IR spectroscopy is the gradual disappearance, at

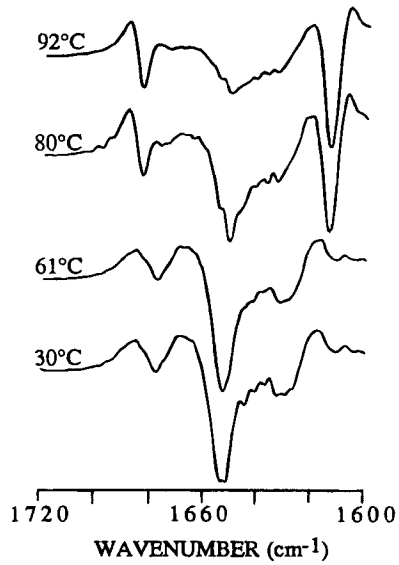

Figure 6—Second-derivative amide I spectra of bovine serum albumin in 50 mM phosphate/D_2O buffer (pD 7.8) recorded at indicated temperatures. Reproduced from Byler and Purcell.[44]

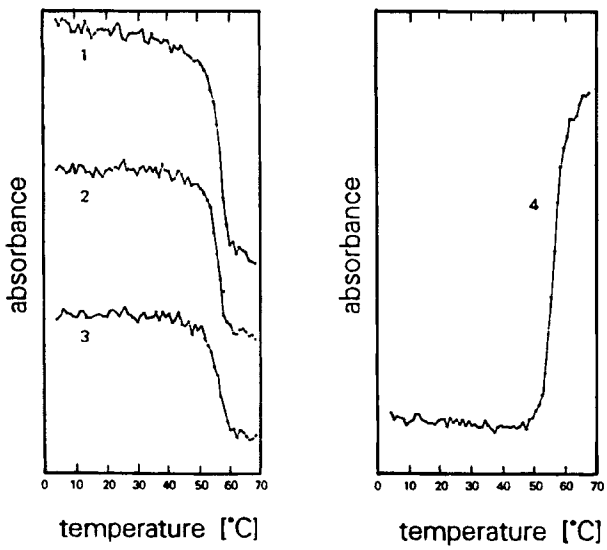

Figure 7—Temperature-dependent behavior of the amide I spectra of acetylcholinesterase in 20 mM phosphate/D_2O buffer (pH 7.4). **(1)** β-sheet band at 1631 cm^{-1}; **(2)** α-helix band at 1648 cm^{-1}; **(3)** α-helix band at 1656 cm^{-1}; **(4)** β-aggregate band at 1622 cm^{-1}. Reproduced from Görne-Tschelnokow et al.[53]

high temperature, of the amide I bands that arise from the ordered secondary structures. A good example of the correlation between the disappearance of native structural bands and the appearance of the intermolecular β-sheet band during thermal denaturation is shown in Figure 7 for acetylcholinesterase.[53] Often coinciding with these spectral transitions is the appearance of a broad and weakly featured band at 1645 cm^{-1}, which can be assigned to unordered structure. An example of this is seen in the FSD spectra of chymotrypsinogen A recorded at various temperatures during thermal unfolding (Figure 8).[49] The spectra obtained between 20 and 46 °C revealed only minor changes in the principal features assigned to different types of secondary structures: α-helix (1652 cm^{-1}), β-sheet (1687, 1637, and 1628 cm^{-1}), turns (1681, 1674, and 1665 cm^{-1}) and unordered (1645 cm^{-1}). Heating the protein solution above 46 °C resulted in a broadening of the overall amide I contour, an increase in the intensity of 1645 cm^{-1} band, and the appearance of sharp bands at 1618 and 1685 cm^{-1}. Concomitant with the appearance of these

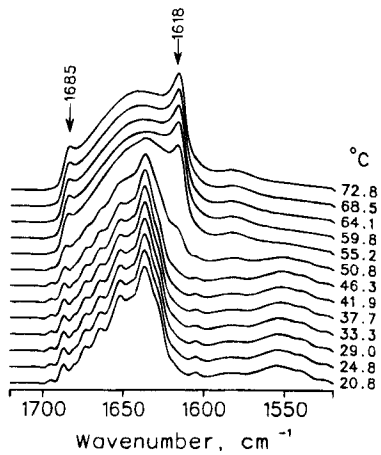

Figure 8—The Fourier self-deconvoluted amide I spectra of chymotrypsinogen A in 10 mM phosphate/D_2O buffer (pH 8.5), recorded as a function of temperatures. The abrupt change in spectra recorded between 50.8 and 55.2 °C is indicative of the irreversible denaturation of the protein. Reproduced from Ismail et al.[49]

bands, the bands associated with native conformation diminished gradually. The blurring of the spectral features of native structures at higher temperature indicated the collapse of ordered secondary structure that results from thermally-induced unfolding and aggregation.

Finally, cold-induced unfolding and aggregation of proteins have also been monitored with FT-IR spectroscopy. Casal and colleagues[57] compared the IR spectra of hemoglobin in the presence or absence of 50% (v/v) glycerol at −100 °C. They found that the overall amide I contours recorded at −100 °C were much broader than those recorded at 25 °C. In the FSD and second-derivative spectra, the intensity of the band at 1622 cm^{-1} increased substantially in hemoglobin at low temperature, with or without glycerol. Other large and reversible changes were observed in hemoglobin in the presence of 50% glycerol, especially the appearance of a new band at 1665 cm^{-1} that was assigned to a distorted α-helical structure.

Lyophilization-Induced Protein Aggregation—*Overview of Structural Studies On Proteins During Dehydration*—As noted in the Introduction, only recently has IR spectroscopy been used to study protein structural transitions during lyophilization. To date, Prestrelski and colleagues[2,3] have reported the effects of drying on the conformations of seven proteins: α-casein, γ-interferon, lactate dehydrogenase (LDH), phosphofructokinase (PFK), α-lactalbumin, basic fibroblast growth factor (bFGF), and granulocyte-colony-stimulating factor (GCSF). Comparisons of the second-derivative spectra of these proteins in the native, aqueous state to that in the dried solid revealed three general responses of proteins to drying: *(1)* the protein maintains the native conformation during dehydration and upon rehydration, as in the case of GCSF; *(2)* the protein unfolds during dehydration but regains the native conformation upon rehydration (reversible unfolding), as observed for α-lactalbumin, and *(3)* the protein unfolds during dehydration and aggregates upon rehydration (irreversible unfolding), as in the case of LDH, PFK, and γ-interferon. Examples of each of these types of transitions are shown in Figure 9.

It is important to stress at this point that although many proteins readily refold, if rehydrated immediately, the unfolded state appears to be much less stable than the native state during long-term storage in the dried solid.[58] Thus, FT-IR spectroscopic analysis of proteins immediately after lyophilization may be useful for predicting storage stability of dried formulations.

Lyophilization-induced protein unfolding/inactivation can be prevented by addition of stabilizers (e.g., sugars) to the

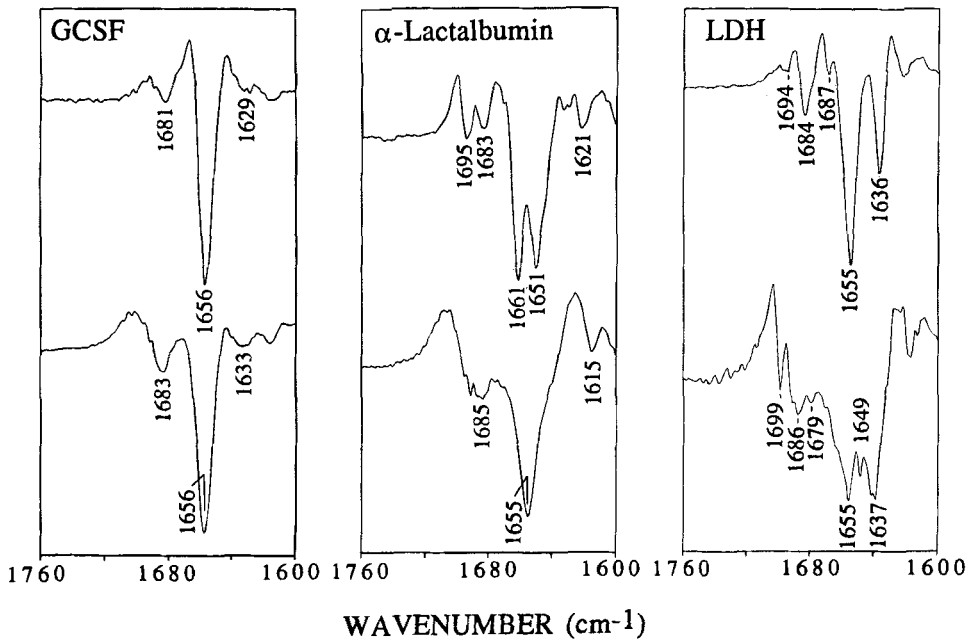

Figure 9—Second-derivative amide I spectra of GCSF, α-lactalbumin, and lactate dehydrogenase in aqueous (upper spectra) and dehydrated (lower spectra) states. Reproduced from Prestrelski et al.[2,3]

Table 2—Spectral Correlation Coefficients and Activity Retention for Lyophilized and Rehydrated Lactate Dehydrogenase and Phosphofructokinase[a]

Condition	LDH	*r*	PFK	*r*
Buffer only	46.1 ± 6.4	0.434	−0.7 ± 0.5	0.830
10 mM Mannitol	39.2 ± 0.1	0.809	4.5 ± 0.4	0.830
10 mM Lactose	43.4 ± 3.4	0.804	5.1 ± 5.0	0.894
10 mM Trehalose	39.0 ± 3.6	0.839	−1.0 ± 0.15	0.862
1% PEG[b]	46.0 ± 0.9	0.776	20.1 ± 0.5	0.876
1% PEG/10 mM Mannitol	80.5 ± 0.8	0.844	30.2 ± 0.7	0.888
1% PEG/10 mM Lactose	100.0 ± 3.5	0.888	102.6 ± 0.0	0.926
1% PEG/10 mM Trehalose	90.1 ± 5.0	0.900	100.0 ± 3.2	0.927

[a] Enzyme activity recovery was expressed as a percentage of prelyophilized activity (data from Prestrelski et al.[2]). [b] PEG, Polyethylene glycol.

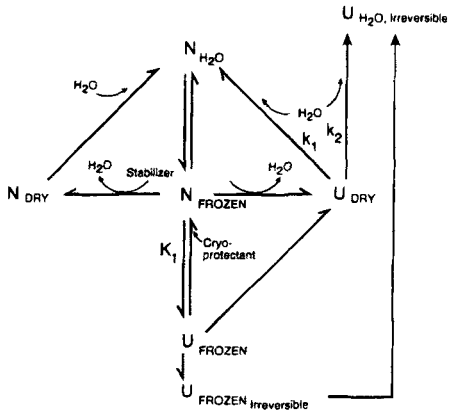

Figure 10—Schematic representation of the conformational transition model of proteins during freezing, drying, and rehydration. Key: (N) native; (U) unfolded: (K_1) conformational equilibrium upon freezing, which shifts toward the native state by addition of cryoprotectant; (k_1) rate constant for refolding; (k_2) rate constant for formation of irreversibly denatured forms. Reproduced from Prestrelski et al.[2]

protein solutions prior to lyophilization. For example, the effects of various additives on the spectral correlation coefficient (comparing dried solid to initial aqueous protein sample) and recovery of enzymatic activities (after rehydration) for LDH and PFK are shown in Table 2.[2] When the enzymes are freeze-dried from the buffer solution alone, there is a high degree of conformational change in both enzymes and a concomitant dramatic loss of enzyme activities upon rehydration. The additives reduced, to varying degrees, the dehydration-induced conformational alterations and loss of enzyme activity. The retention of the native structure in the dried solid and recovery of activity were greatest in the presence of a combination of polyethylene glycol (which protects specifically during freezing) and a sugar (which at the concentrations tested protects only during drying). Neither the sugar nor polyethylene glycol alone, at the concentrations studied, protected against lyophilization-induced unfolding/inactivation. These results demonstrate clearly that the inhibition of aggregation and recovery of activity of labile enzymes after rehydration correlates directly with retention of the native structure in the dried solid, and that for optimum stabilization a protein must be protected specifically during both freezing and drying stresses.

Based on their results with stress-specific stabilization, Prestrelski, Arakawa, and Carpenter[1,2] have proposed a conformational transition model that describes the structural transitions in proteins during lyophilization. As shown in Figure 10, beginning with a native protein in aqueous solution (N_{H2O}), freezing in the absence of a cryoprotectant results in a non-native conformation in dried state (U_{frozen}). Drying from this point results in a non-native conformation in the dried state (U_{dry}). In contrast, freezing in the presence of a cryoprotectant results in preservation of the native structure in the frozen state (N_{frozen}). However, if the cryoprotectant does not also protect during subsequent drying, a non-native structure (U_{dry}) will be obtained in dried solid. Conversely, a stabilizer that can serve as a water substitute and hydrogen bond to the protein will preserve the native structure during subsequent drying. Starting with N_{frozen}, use of the latter type of stabilizer should lead to formation of N_{dry}.

To test the validity of this model, however, we need not only the data from the studies of protein conformations in aqueous and dried states, in the presence or absence of stabilizers (e.g., polyethylene glycol and sugar, alone and in combination), but also the data on protein conformations in the frozen state. The latter can be provided by a low-temperature-attenuated total reflectance IR accessory, which was recently developed

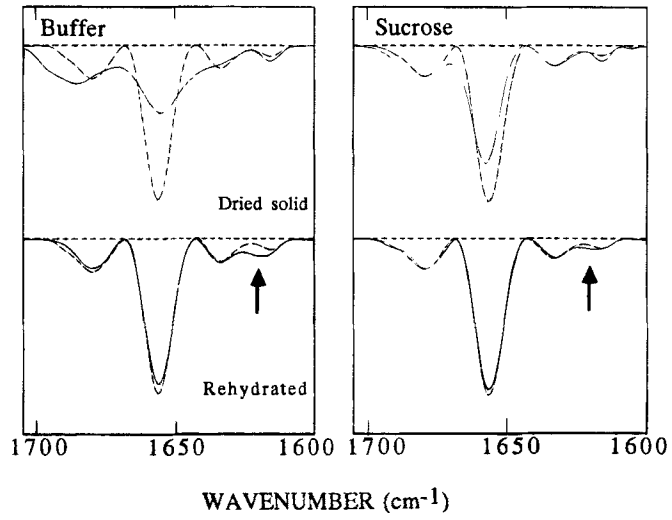

Figure 11—Comparisons of second-derivative spectra of γ-interferon in dried solid and rehydrated states, with or without 1 M sucrose, with the spectrum of aqueous native state. γ-Interferon (28.5 mg/mL) is in 100 mM Tris-HCl buffer (pH 7.3). The spectra of the native state are shown in dashed lines. The arrows show the band arising from non-native β-sheet structure (Dong, A.; Prestrelski, S. J.; Arakawa, T.; Carpenter, J. F., unpublished data).

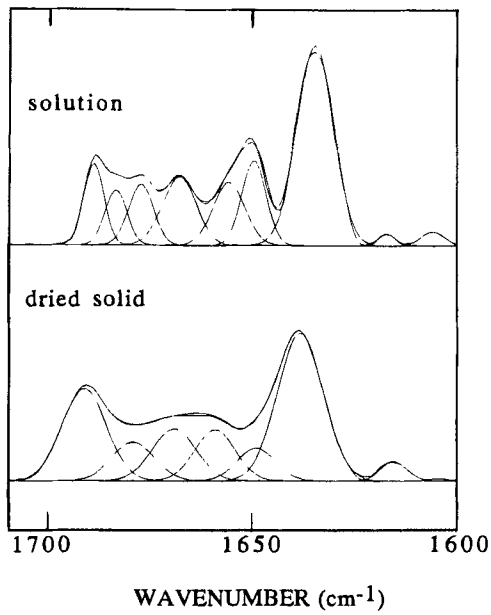

Figure 12—Curve-fitted inverted second-derivative spectra of chymotrypsinogen A in aqueous native and dried states: (upper panel) aqueous native state, (lower panel) dried solid (Allison, S. D.; Dong, A.; Carpenter, J. F., unpublished results).

by Remmele and Stushnoff.[59,60] This new accessory permits one to monitor the structural changes of a protein throughout the entire freeze-drying cycle. This approach should provide new insights into the mechanism of protein damage and stabilization during freezing and subsequent drying.

Finally, one concern that arises with the IR study of dried protein formulations is the potential contribution of residual water to the absorbance in the amide I region. In studies with numerous different dried protein formulations, we have not noted any significant interference from residual water. The H_2O band at 1640 cm^{-1} is extremely broad relative to the widths of the protein bands, which greatly reduces the relative intensity of the H_2O band in second-derivative spectra of proteins. Therefore, even in dried protein samples containing up to 10% (w/w) residual water, the H_2O band does not appear in the amide I second-derivative spectrum.[61]

Studies Specifically Related to Lyophilization-Induced Aggregation—Based on the data presently available, we propose that the degree of aggregation noted after rehydration will correlate directly with the degree to which the protein sample is unfolded in the dried solid. According to this hypothesis, minimizing aggregation after rehydration is directly dependent on maximizing retention of native structure during freezing and drying. Our results with γ-interferon provide a preliminary test of this hypothesis. The second-derivative spectra for γ-interferon, which was lyophilized in the absence or presence of 1 M sucrose, in the initial aqueous solution, in the dried solid, and after rehydration are shown in Figure 11. The spectrum of γ-interferon dried without sucrose shows marked loss of native structure, whereas the spectrum of the protein dried with sucrose shows considerable resemblance to the spectrum of native state. The correlation coefficients (r) relative to the native, aqueous protein are 0.706 and 0.925, respectively, for the samples dried without and with sucrose. After rehydration, the spectra of both samples are very native-like, indicating that the majority of non-native molecules have refolded ($r = 0.802$ without sucrose and 0.998 with sucrose). However, in the sample lyophilized without sucrose, the appearance of a new band near 1625 cm^{-1}, which is assignable to intermolecular β-sheet structure, and the decreased intensities in vibrational bands ascribed to α-helix (1656 cm^{-1}) and turn (1688–1665 cm^{-1}) structures indicate the formation of protein aggregates upon rehydration. In this sample, 18% of the protein formed insoluble aggregates. In contrast, in the sample lyophilized with sucrose, only 9% insoluble aggregate was noted after rehydration. This reduction in aggregation is reflected in a much weaker 1625 cm^{-1} band in the spectrum of the rehydrated sample. In this case, 1 M sucrose does not provide complete protection during freeze-drying, presumably because it is inadequate at preserving the protein structure during the freezing step. However, these result do support the contention that maintaining the native conformation of a protein in the dried state is related directly to minimizing aggregation upon rehydration.

Chymotrypsinogen A (CTG) is another useful model protein with which to study the connection between the degree of lyophilization-induced unfolding of a protein sample and the degree of aggregation measured after rehydration. In this case, the protein sample unfolds during lyophilization (see Figure 12), but refolds completely during rehydration (data not shown). The correlation coefficient for the protein spectrum in the dried solid relative to that in the initial aqueous state is 0.664. The value for the rehydrated sample is 0.999. This experiment actually provides an interesting example of the different types of information available from a global quantitative comparison of spectra by correlation coefficient analysis versus that obtained from quantitation of secondary structure. Even though the correlation coefficient indicates that the protein was clearly non-native in the dried solid, the actual proportions of secondary structural types are essentially unchanged (Table 3). The latter observation is due to the fact that bands were shifted to new positions in the dried sample, but these positions can be assigned to the same secondary structures as those noted in the aqueous protein. For example, there are several component bands under the amide I contour that are assigned to β-sheet structure (see Table 3). Therefore, although it is of great interest to know the secondary structure of proteins in various states, the correlation coefficient provides a more reliable estimate for the overall degree of structural similarity to a reference state.

Refolding of CTG could be dominant during rehydration either because the protein is intrinsically resistant to aggregation under the present experimental conditions (e.g., due to electrostatic repulsion between protein molecules) or because the degree of unfolding in the protein population was

Table 3—Assignments and Relative Areas of Amide I Components of Chymotrypsinogen in Aqueous Native and Dried States in the Presence or Absence of Thiocyanate

Aqueous		Dried		Dried/0.25 M SCN		Dried/1.0 M SCN		
ν (cm^{-1})	A (%)	ν (cm^{-1})	A (%)	ν (cm^{-1})	A (%)	ν (cm^{-1})	A (%)	Assignment
1616[b]	—	1615	1.2	1615	6.9	1615	19.2	Inter β[c]
—	—	—	—	—	—	1627	8.0	Inter β
1635	40.3	1638	36.6	1639	27.6	1639	8.8	Intra β[d]
1649	11.5	1649	7.0	1649	0.9	1648	8.4	Unordered
1656	11.3	1659	11.3	1658	14.0	1658	11.0	α-helix
1668	12.7	1669	12.3	1669	13.8	1669	14.7	Turn
1677	8.3	1679	9.0	1681	10.5	1680	7.9	Turn
1683	6.6	—	—	—	—	—	—	Turn
1689	9.4	1691	22.6	1691	14.4	1691	9.9	Intra β
—	—	—	—	1699	11.9	1698	12.1	Inter β

[a] Relative band areas determined by curve-fitting analysis. [b] The weak 1616 cm^{-1} band in aqueous native state that arises from side-chain vibration is not included in secondary structure estimation. It has also been subtracted from the overlapping band at 1615 cm^{-1}. [c] Inter β, Intermolecular β-sheet. [d] Intra β, Intramolecular β-sheet.

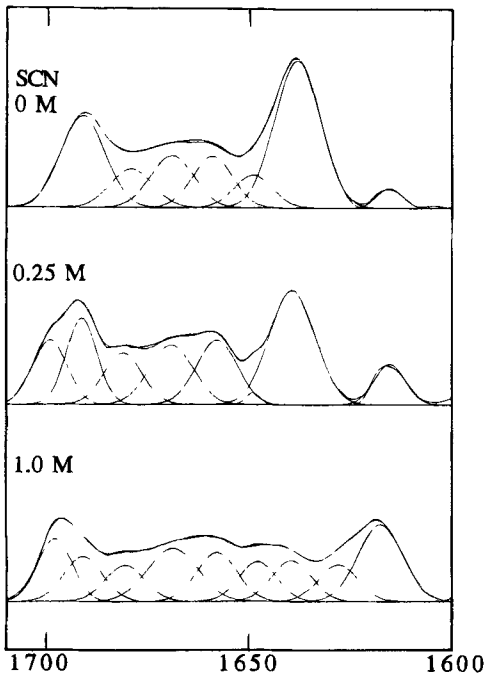

Figure 13—Curve-fitted inverted second-derivative spectra of chymotrypsinogen A in dried solid with or without thiocyanate (Allison, S. D.; Dong, A.; Carpenter, J. F., unpublished results).

not sufficient to favor aggregation during rehydration. To distinguish between these possibilities, we have lyophilized the protein in the presence of thiocyanate. This destabilizer should increase the degree of lyophilization-induced unfolding in the protein sample. As shown in Figure 13, lyophilizing the protein in the presence of 0.25 M thiocyanate greatly increases the structural perturbation noted in the dried solid, as indicated by a correlation coefficient of 0.404 relative to the initial native state. When this sample is rehydrated, 81% of the protein forms insoluble aggregates. This level of thiocyanate does not significantly alter structure in solution, nor induce aggregation, prior to lyophilization (data not shown). These results demonstrate that CTG can be induced to aggregate during freeze-drying and rehydration, if the degree of unfolding is high enough in the dried protein sample.

Finally, comparing the data for CTG freeze-dried alone or with 0.25 M thiocyanate with those for the protein freeze-dried in the presence of 1 M thiocyanate provides an interesting example of the useful information that can be obtained from quantitative determination of protein secondary structural content (Figure 13). The protein prepared in the presence of 1 M thiocyanate is >90% aggregated prior to lyophilization and fully aggregated upon rehydration. Thus, the spectrum of the protein in the dried solid can be used as an estimate of that for a fully aggregated, dried sample. First, the overall spectrum is grossly perturbed; that is, $r = -0.021$ versus native aqueous CTG. More importantly, bands indicative of intermolecular β-sheet structure (i.e., bands at 1615, 1627, and 1698 cm^{-1}) account for ~39% of the total secondary structure (Table 3). The appearance of the same bands in the spectrum for the protein lyophilized in the presence of 0.25 M thiocyanate indicates that some degree of aggregation had occurred prior to rehydration. With the data available from curve-fitting and quantitation of secondary structure, we can estimate the degree of aggregation in the dried solid. First, we must assume that the sample lyophilized in the presence of 1 M thiocyanate can be used as a reference for 100% aggregation in the dried solid (i.e., 39.3% intermolecular β-sheet equals 100% aggregation). The sample freeze-dried in the presence of 0.25 M thiocyanate contains 18.8% intermolecular β-sheet, which is equivalent to 47.8% aggregation in the dried solid. The level of aggregation increases to 81% in the rehydrated sample, so we conclude that many of the unfolded molecules do not aggregate until the addition of water to the sample.

Conclusions

We are just beginning to understand lyophilization-induced protein structural transitions and their inhibition by stabilizers. However, it is already clear that to recover biological activities upon rehydration, proteins must be stabilized against both the freezing and drying stresses during lyophilization. Also, it appears that the minimum criterion for a successful lyophilized protein formulation is the preservation of the native conformation in the dried solid. Due to its high sensitivity to structural changes of proteins under broad range of physical conditions, FT-IR spectroscopy is proving to be an invaluable tool for study lyophilization-induced unfolding and aggregation of proteins. The strong band near 1620 cm^{-1} and associated weak band near 1685 cm^{-1} in D_2O (or higher wavenumbers in H_2O), which are indicative of intermolecular β-sheet, are common IR spectral features for both lyophilization- and temperature-induced protein aggregation. Thus, these bands can be used to monitor and quantify aggregation, even in the dried solid. Finally, a newly developed IR accessory[59,60] provides new opportunities to study the conformational transitions in proteins during the entire freeze-drying cycle. Thus, the optimization of formulations will be a straightforward, rational process, because the researcher will be able to assess directly the capacity of additives to preserve native structure during both freezing and drying.

References and Notes

1. Carpenter, J. F.; Prestrelski, S. J.; Arakawa, T. *Arch. Biochem. Biophys.* **1993**, *303*, 456–464.
2. Prestrelski, S. J.; Arakawa, T.; Carpenter, J. F. *Arch. Biochem. Biophys.* **1993**, *303*, 465–473.
3. Prestrelski, S. J.; Tedeschi, N.; Arakawa, T.; Carpenter, J. F. *Biophys. J.* **1993**, *65*, 661–671.
4. Arakawa, T.; Prestrelski, S. J.; Kenney, W. C.; Carpenter, J. F. *Adv. Drug Delivery Rev.* **1993**, *10*, 1–28.
5. Rupley, J. A.; Careri, G. *Adv. Protein Chem.* **1991**, *41*, 37–172.

6. Kuntz, I. D.; Kauzmann, W. *Adv. Protein Chem.* **1974**, *28*, 239–345.
7. Edsall, J. T.; McKenzie, H. A. *Adv. Biophys.* **1983**, *16*, 53–183.
8. Susi, H.; Byler, D. M. *Methods Enzymol.* **1986**, *130*, 290–311.
9. Surewicz, W. K.; Mantsch, H. H. *Biochim. Biophys. Acta* **1988**, *952*, 115–130.
10. Prestrelski, S. J.; Williams, A. L.; Liebmam, M. *Proteins*, **1992**, *14*, 430–439.
11. Prestrelski, S. J.; Byler, D. M.; Liebmam, M. *Proteins*, **1992**, *14*, 440–450.
12. Dong, A.; Caughey, W. S. *Methods Enzymol.* **1994**, *232*, 139–175.
13. Koenig, J. L.; Tabb, D. L. In *Analytical Applications of FT-IR to Molecular and Biological Systems*; Durig, J. R. Ed.; Reidel: Dordrecht, 1980; pp 241–255.
14. Parker, F. S. *Applications of Infrared, Raman and Resonance Raman Spectroscopy in Biochemistry*; Plenum: New York, 1983.
15. Clark, A. H.; Saunderson, D. P. H.; Suggett, A. *Int. J. Pept. Protein Res.* **1981**, *17*, 353–364.
16. Caughey, B. W.; Dong, A.; Bhat, K. S.; Ernst, D.; Hayes, S. F.; Caughey, W. S. *Biochemistry* **1991**, *30*, 7672–7680.
17. Krimm, S.; Bandekar, J. *Adv. Protein Chem.* **1986**, *38*, 181–364.
18. Bandekar, J. *Biochem. Biophys. Acta* **1992**, *1120*, 123–143.
19. Susi, H. In *Structure and Stability of Biological Macromolecules*; Timasheff, S. N.; Fasman, G. D., Eds.; Marcel Dekker: New York, 1969; pp 575–663.
20. Arrondo, J. L. R.; Muga, A.; Castresana, J.; Goni, F. *Prog. Biophys. Mol. Biol.* **1993**, *59*, 23–56.
21. Stone, H. *J. Opt. Soc. Am.* **1962**, *52*, 998–1003.
22. Kauppinen, J. K.; Moffatt, D. J.; Mantsch, H. H.; Cameron, D. G. *Appl. Spectrosc.* **1981**, *35*, 271–276.
23. Kauppinen, J. K.; Moffatt, D. J.; Mantsch, H. H.; Cameron, D. G. *Anal. Chem.* **1981**, *53*, 1454–1457.
24. Susi, H.; Byler, D. M. *Biochem. Biophys. Res. Commun.* **1983**, *115*, 391–397.
25. Cameron, D. G.; Moffatt, D. J. *Appl. Spectrosc.* **1987**, *41*, 539–544.
26. Mantsch, H. H.; Moffatt, D. J.; Casal, H. L. *J. Mol. Struct.* **1988**, *173*, 285–298.
27. Dong, A.; Huang, P.; Caughey, W. S. *Biochemistry* **1992**, *31*, 182–189.
28. Byler, D. M.; Susi, H. *Biopolymers* **1986**, *25*, 469–487.
29. Dong, A.; Caughey, B.; Caughey, W. S.; Bhat, K. S.; Coe, J. E. *Biochemistry* **1992**, *31*, 9364–9370.
30. Dong, A.; Caughey, W. S.; Du Clos, T. W. *J. Biol. Chem.* **1994**, *269*, 6424–6430.
31. Dong, A.; Huang, P.; Caughey, W. S. *Biochemistry* **1990**, *29*, 3303–3308.
32. Papiz, M. Z.; Sawyer, L.; Eliopoulos, E. E.; North, A. C. T.; Findlay, J. B. C.; Sivaprasadarao, R.; Jones, T. A.; Newcomer, M. E.; Kraulis, P. J. *Nature* **1986**, *324*, 383–385.
33. Monaco, H. L.; Zanotti, G.; Spadon, P.; Bolognesi, M.; Sawyer, L.; Eliopoulos, E. E. *J. Mol. Biol.* **1987**, *197*, 695–706.
34. Cameron, D. G.; Moffatt, D. J. *J. Test Eval.* **1984**, *12*, 78–85.
35. Surewicz, W. K.; Mantsch, H. H.; Chapman, D. *Biochemistry* **1993**, *32*, 289–394.
36. Dong, A.; Huang, B.; Caughey, B.; Carpenter, J. F.; Caughey, W. S., unpublished results.
37. Dong, A.; Prestrelski, S. J.; Carpenter, J. F., unpublished results.
38. Levitt, M.; Greer, J. *J. Mol. Biol.* **1977**, *114*, 181–293.
39. Clark, A. H.; Tuffnell, C. D. *Int. J. Pept. Protein Res.* **1980**, *16*, 339–351.
40. Miyazawa, T.; Blout, E. R. *J. Am. Chem. Soc.* **1962**, *83*, 712–719.
41. Krimm, S. *J. Mol. Biol.* **1962**, *4*, 528–540.
42. Susi, H.; Timasheff, S. N.; Stevens, L. *J. Biol. Chem.* **1967**, *242*, 5467–5473.
43. Casal, H. L.; Köhler, U.; Mantsch, H. H. *Biochim. Biophys. Acta* **1988**, *957*, 11–20.
44. Byler, D. M.; Purcell, J. M. *SPIE Fourier Transform Spectrosc.* **1989**, *1145*, 415–417.
45. Surewicz, W. K.; Scabo, A.; Mantsch, H. H. *Eur. J. Biochem.* **1987**, *167*, 519–523.
46. Surewicz, W. K.; Leddy, J. J.; Mantsch, H. H. *Biochemistry* **1990**, *29*, 8106–8111.
47. Labruyere, E.; Mock, M.; Surewicz, W. K.; Mantsch, H. H.; Rose, T.; Munier, H.; Sarfati, R. S.; Barzu, O. *Biochemistry* **1991**, *30*, 2619–2624.
48. Muga, A.; Mantsch, H. H.; Surewicz, W. K. *Biochemistry* **1991**, *30*, 7219–7224.
49. Ismail, A. A.; Mantsch, H. H.; Wong, P. T. T. *Biochim. Biophys. Acta* **1992**, *1121*, 183–188.
50. Jackson, M.; Mantsch, H. H. *Biochim. Biophys. Acta* **1992**, *1118*, 139–143.
51. Naumann, D.; Schultz, C.; Gorne-Tschelnokow, U.; Hucho, F. *Biochemistry* **1993**, *32*, 3162–3168.
52. Urbanova, M.; Pancoska, P.; Keiderling, T. A. *Biochim. Biophys. Acta* **1993**, *1203*, 290–294.
53. Görne-Tschelnokow, U.; Naumann, D.; Weise, C.; Hucho, F. *Eur. J. Biochem.* **1993**, *213*, 1235–1242.
54. Tanfani, F.; Bertoli, E.; Signoini, M.; Bergamini, C. M. *Eur. J. Biochem.* **1993**, *218*, 499–505.
55. Fabian, H.; Schultz, C.; Naumann, D.; Landt, O.; Hahn, U.; Saenger, W. *J. Mol. Biol.* **1993**, *232*, 967–981.
56. Seshadri, S.; Oberg, K. A.; Fink, A. L. *Biochemistry* **1994**, *33*, 1351–1355.
57. Casal, H. L.; Köhler, U.; Mantsch, H. H.; Goni, F. M.; Arrondo, J. L. R. *Z. Naturforsch. C: Biosci.* **1987**, *42*, 1339–1342.
58. Prestrelski, S. J.; Chang, B., unpublished results.
59. Remmele, R. L., Jr.; Stushnoff, C. *Biopolymers* **1994**, *34*, 365–370.
60. Remmele, R. L., Jr.; Stushnoff, C.; Carpenter, J. F. *American Chemical Society Symposium Series* **1994**, *567*, 170–192.
61. Prestrelski, S. J., unpublished results.

Acknowledgments

We gratefully acknowledge support from the Office of Naval Research (Grant N00014-94-1-0402) to J.F.C. and an American Foundation for Pharmaceutical Education Graduate Fellowship to S.D.A.

JS940557A